



Met Office
Hadley Centre

Food insecurity and climate change technical report

November 2015



This document is published by the Met Office on behalf of the Secretary of State for Business, Innovation and Skills, HM Government, UK. Its content is covered by © Crown Copyright 2015.

The Met Office aims to ensure that the content of this document is accurate and consistent with its best current scientific understanding. However, the science which underlies meteorological forecasts and climate projections is constantly evolving. Therefore, any element of the content of this document which involves a forecast or a prediction should be regarded as our best possible guidance, but should not be relied upon as if it were a statement of fact. To the fullest extent permitted by applicable law, the Met Office excludes all warranties or representations (express or implied) in respect of the content of this document.

Use of the content of this document is entirely at the reader's own risk. The Met Office makes no warranty, representation or guarantee that the content of this document is error free or fit for your intended use.

Before taking action based on the content of this document, the reader should evaluate it thoroughly in the context of his/her specific requirements and intended applications.

To the fullest extent permitted by applicable law, the Met Office, its employees, contractors or subcontractors, hereby disclaim any and all liability for loss, injury or damage (direct, indirect, consequential, incidental or special) arising out of or in connection with the use of the content of this document including without limitation any and all liability:

- relating to the accuracy, completeness, reliability, availability, suitability, quality, ownership, non-infringement, operation, merchantability and fitness for purpose of the content of this document;
- relating to its work procuring, compiling, interpreting, editing, reporting and publishing the content of this document; and
- resulting from reliance upon, operation of, use of or actions or decisions made on the basis of, any facts, opinions, ideas, instructions, methods, or procedures set out in this document.

This does not affect the Met Office's liability for death or personal injury arising from the Met Office's negligence, nor the Met Office's liability for fraud or fraudulent misrepresentation, nor any other liability which cannot be excluded or limited under applicable law.

If any of these provisions or part provisions are, for any reason, held to be unenforceable, illegal or invalid, that unenforceability, illegality or invalidity will not affect any other provisions or part provisions which will continue in full force and effect.

Contents

1	Introduction	3
2	Vulnerability to food insecurity in the present-day.....	3
2.1	The baseline exposure component	3
2.2	The baseline sensitivity and adaptive capacity components.....	6
2.3	The baseline climate and food insecurity index	7
3	Future projections of vulnerability to food insecurity	8
3.1	Greenhouse gas emission scenarios.....	8
3.2	Scenarios of adaptation investment.....	10
3.3	The future climate and food insecurity index	11
4	References.....	12

1 Introduction

The Food Insecurity & Climate Change website (www.wfp.org/climate-food-insecurity-index or www.metoffice.gov.uk/food-insecurity-index) showcases an interactive climate and food insecurity index which allows the user to explore policy outcomes for vulnerability to food insecurity. The website shows a present-day measure of vulnerability of the food system to climate-related hazards, and future projections of the index for a range of scenarios of different future global greenhouse gas emissions and adaptation levels.

This technical report gives detail about the calculation of the baseline index in Section 2, and the future projections of the index in Section 3.

2 Vulnerability to food insecurity in the present-day

The baseline climate and food insecurity index is a relative measure of the present-day vulnerability to food insecurity, based on an adaptation of the Hunger and Climate Vulnerability Index (HCVI) from Krishnamurthy *et al.* (2014).

Vulnerability to food insecurity is calculated at a country level and is comprised of three equally weighted, normalised components (as in Krishnamurthy *et al.* (2014)):

- **Exposure** to climate-related hazards,
- **Sensitivity** of national agricultural production to climate-related hazards,
- **Adaptive capacity** - a measure of capacity to cope with climate-related food shocks.

Each of these components is made up of country-level indicators, selected based on their relevance to food security and their correlation with the FAO measure of undernutrition (FAO, 2014).

The climate and food insecurity index used in this study is an adapted version of the HCVI, where the exposure component has been replaced with a measure of exposure from gridded meteorological data. This allows future projections of the vulnerability index using climate model projections (see Section 3.1). Future projections of the sensitivity and adaptive capacity components of the index are also explored through scenarios of different adaptation levels (see Section 3.2).

OECD and EU countries are excluded from the index calculation. Access to markets and economic interconnectedness in the most developed countries means they have a different food security profile and are not affected by climate risks in the same way as the least-developed countries which rely more heavily on in-country food production. In addition, small countries (< 500 km²) are excluded for resolution reasons.

2.1 The baseline exposure component

The exposure component in the original HCVI included observational data on the number of floods, droughts and storms, and indicators of the number of deaths and economic losses due to climate-related disasters, from a self-reporting database¹. However, as information about the future climate comes from gridded climate model data, it was necessary to adapt the baseline climate exposure component so that it also includes gridded data. This is to ensure that comparisons of the index between the future and present day are fair. Not all of the indicators used to represent exposure in the original HCVI are able to be reproduced from climate model output, i.e. the number

¹ EM-DAT – The International Disaster Database (<http://www.emdat.be/>)

of deaths and economic losses due to climate-related disasters, as they are also partially driven by socio-economic factors and are therefore not possible to recreate from analysis of climate model data. As it would be inconsistent to keep these indicators constant while considering the projected changes in climate-related disasters, both the number of deaths and economic losses due to climate-related disasters are not included in this gridded-data adjusted exposure component.

The gridded-data adjusted measure of exposure to climate-related hazards is represented as a measure of the average length of drought and flood events per country. Drought and flood indicators were constructed over the 1981-2010 baseline period from the WATCH Forcing Dataset (Wheedon *et al.*, 2011); a gridded (0.5° resolution) meteorological dataset of present-day climate. The WATCH forcing data was regridded using bilinear interpolation to a 90 x 144 grid for compatibility with the climate model output used to compute the future projections of the exposure component (see Section 3.1).

Other indicators were tested but failed to pass the criteria for inclusion in the index; indicators of extreme temperature from the WATCH data did not correlate with undernutrition, and attempts to create a storm indicator from both the WATCH data and the IBTrACs dataset (Knapp *et al.*, 2010) were unsuccessful.

Drought indicator

The drought indicator utilised an adapted version of the Moving Average Precipitation Variable Threshold (MAPVT) indicator (Wanders *et al.* 2010). The MAPVT uses the 30-day rolling average precipitation amount throughout the 30-year baseline period to calculate the 20th percentile for each month and grid cell. This value represents the threshold for determining if a day is within a drought event. The calculated thresholds are then utilised to identify drought events, defined as two consecutive days in which the daily rainfall amount was less than the drought threshold for that month, throughout the time series, at each grid cell. Any daily rainfall amounts less than 1 mm are removed; this is a standard processing technique to address the well known problem that numerical models over-represent precipitation at low intensities (Sun *et al.*, 2005).

The MAPVT utilised in this study is adapted to better represent realistic conditions; one significant issue was that one day of sufficient rainfall could end a long or very severe drought event. In this study, a drought event begins when the daily rainfall is below the threshold defined above, and ends when rainfall exceeds the *cumulative* deficit (the daily amount less than the daily drought threshold). No assumptions were made regarding the soil moisture, hydrological conditions or runoff characteristics of the land within a grid cell.

The indicator for the average length of drought events was chosen to be used in the exposure component as it had the strongest correlation value with undernutrition (after masking and aggregating the data to country borders – see later sections). The spatial pattern of the average length of drought events indicator is shown in Figure 1 (left panel).

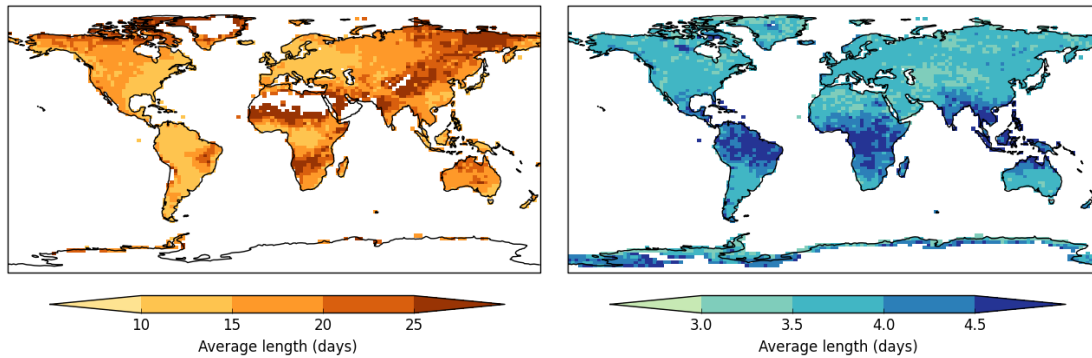


Figure 1 – Spatial patterns of the ‘average length of drought events’ (days, left) and ‘average length of flood events’ (% , right) indicators from the WATCH dataset for 1981-2010.

Flood indicator

A further adaptation of the MAPVT indicator was utilised to construct a flood indicator based on periods of excess rainfall. The 5-day rolling average rainfall is assessed to identify the 95th percentile for each 5-day period within the year (i.e. each day of year ± 2 days), throughout the 30-year baseline period. The 5-day rolling average is utilised instead of the 30-day period for drought, due to the shorter time scales associated with flood events and to remove the impact of strong seasonal changes in rainfall for some locations (e.g. monsoons).

Similar to the drought indicator, an excess water event was only deemed to end once the rainfall amount was low enough to overcome the excess rainfall over the period. Furthermore, the exception that two days of no rainfall indicates the end of any excess water periods was included, this was to make some allowance for the fact that water can drain away or evaporate over a period.

The indicator for the average length of flood events was chosen to be used in the exposure component as it had the strongest correlation value with undernutrition (after masking and aggregating the data to country borders – see later sections). The spatial pattern of the average length of flood events indicator is shown in Figure 1 (right panel).

Different flood metrics were tested, including the number of days of excess rainfall, the number of discrete excess rainfall events, the severity of flood events (cumulative amount of rainfall within the event above the daily threshold level, in mm) and the percentage severity of excess rainfall events (the proportion of the calculated severity to the threshold amount (i.e. 110% means an event with 10% more rainfall over the event threshold)).

Masking the data

In order to create a measure of exposure, rather than just an indicator of meteorological floods and droughts, the data was masked to only include regions with a population density greater than 150 people per km² (definition of rural population based on OECD (2011), using an estimate of population density in the year 2000 (van Vuuren *et al.*, 2007)) and with more than 1% of the grid cell given over to crop production (using cropland data representative of the year 2000 from Monfreda *et al.*, 2008), shown in Figure 2.

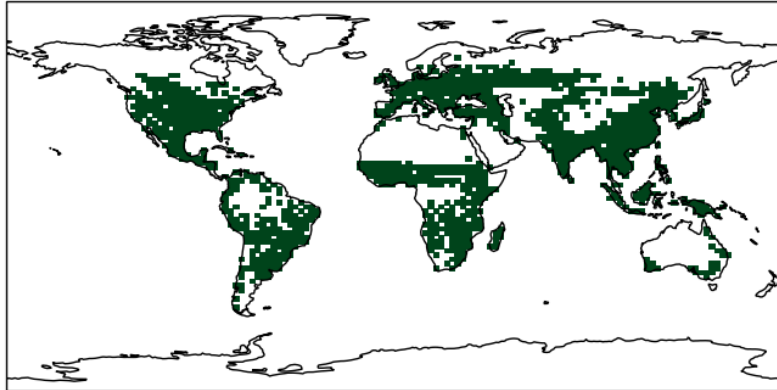


Figure 2 – Mask applied to gridded data. Grid cells used in the calculation are shown in green. These are the grid cells where the population density is greater than 150 people per km² and more than 1% of the grid cell is cropland.

Aggregation to country borders

The average length of flood and drought indicators were aggregated to country-level indices by selecting the median value within a country's borders (calculated using the Natural Earth² dataset and Iris³). The countries excluded from the vulnerability index calculation (OECD and EU countries, and countries less than 500 km²) were also excluded from the exposure calculation. Note that countries with no exposure component (due to the application of the population and cropland mask) were also excluded from the vulnerability index calculation.

Calculating the exposure component

Once the necessary countries were excluded, the average length of flood and drought events indicators were normalised with respect to their maximum and minimum values, resulting in a relative measure of the average length of floods and droughts between countries. The exposure component was then calculated by summing the flood and drought indicators and again normalising with respect to the maximum and minimum values, resulting in a relative measure of exposure to flood and drought events on a scale of 0 to 1.

2.2 The baseline sensitivity and adaptive capacity components

The baseline sensitivity and adaptive capacity components of the vulnerability index are represented by country-level indicators that correlate with undernutrition representative of the year 2010⁴. These are the same indicators that were used in the original HCVI, and are shown in Table 1 (see Krishnamurthy *et al.* (2014) for further detail on data sources).

The sensitivity and adaptive capacity components were constructed by normalising the indicator values with respect to plausible maximum and minimum values for each of the datasets (shown in Table 1). Indicators marked with a * in Table 1 correlate negatively with undernutrition (FAO, 2014), and are therefore inverted at this stage. The sensitivity and adaptive capacity components are then calculated by taking the average value across the indicators (three indicators for sensitivity and eight for adaptive capacity, see

² <http://www.naturalearthdata.com/>

³ <http://scitools.org.uk/iris/>

⁴ The sensitivity and adaptive capacity indicator values for South Sudan were set to be the same as those for Sudan as South Sudan gained independence from Sudan in 2011, after these data were collected.

Table 1). This results in sensitivity and adaptive capacity values for each country that exist on a 0 to 1 scale, where 0 represents the lowest plausible sensitivity and highest plausible adaptive capacity values, and 1 represents the highest plausible sensitivity and lowest plausible adaptive capacity values.

Table 1 – Indicators used in the sensitivity and adaptive capacity components, their data source and the plausible maximum and minimum values from the datasets. Indicators marked * correlate negatively with undernutrition (FAO, 2014).

Component	Indicator	Data source	Plausible maximum value	Plausible minimum value
Sensitivity	Forest cover (% of total area)*	World Bank Data	95%	0%
	Rainfed agriculture (% of total agriculture),	World Resources Institute	100%	0%
	Cereal crop yield (tons/ha)*	FAOSTAT	8000 tons/ha	300 tons/ha
Adaptive capacity	Water access (rural population) (%)*	World Bank Data	100%	10%
	Water access (urban population) (%)*	World Bank Data	100%	35%
	Paved roads (% of all roads)*	World Bank Data	100%	1%
	Government effectiveness (%)*	World Bank Governance Data	100%	0%
	Decadal population growth (2000-2010) (%)	UNFPA	4%	0%
	Total population below poverty line (\$2 per day, PPP) (%)	UNDP	75%	0%
	Vulnerable employment (% of total labour force)	World Bank Data	90%	0%
	Rural population (% of total population)	World Bank Data	90%	0%

The sensitivity and adaptive capacity components were constructed by normalising the indicator values with respect to plausible maximum and minimum values for each of the datasets (shown in Table 1). Indicators marked with a * in Table 1 correlate negatively with undernutrition (FAO, 2014), and are therefore inverted at this stage. The sensitivity and adaptive capacity components are then calculated by taking the average value across the indicators (three indicators for sensitivity and eight for adaptive capacity, see Table 1). This results in sensitivity value and adaptive capacity values for each country that exists on a 0 to 1 scale, where 0 represents the lowest plausible sensitivity and highest plausible adaptive capacity values, and 1 represents the highest plausible sensitivity and lowest plausible adaptive capacity values.

2.3 The baseline climate and food insecurity index

Following the methodology in Krishnamurthy *et al.* (2014), the exposure, sensitivity and adaptive capacity indicators defined above were summed and normalised with respect to the maximum and minimum values to create a scaled country-level index on a scale of 0 to 1. This present-day measure of vulnerability to food insecurity is shown in Figure 3, and it can be seen that the most vulnerable countries are located in sub-Saharan Africa.

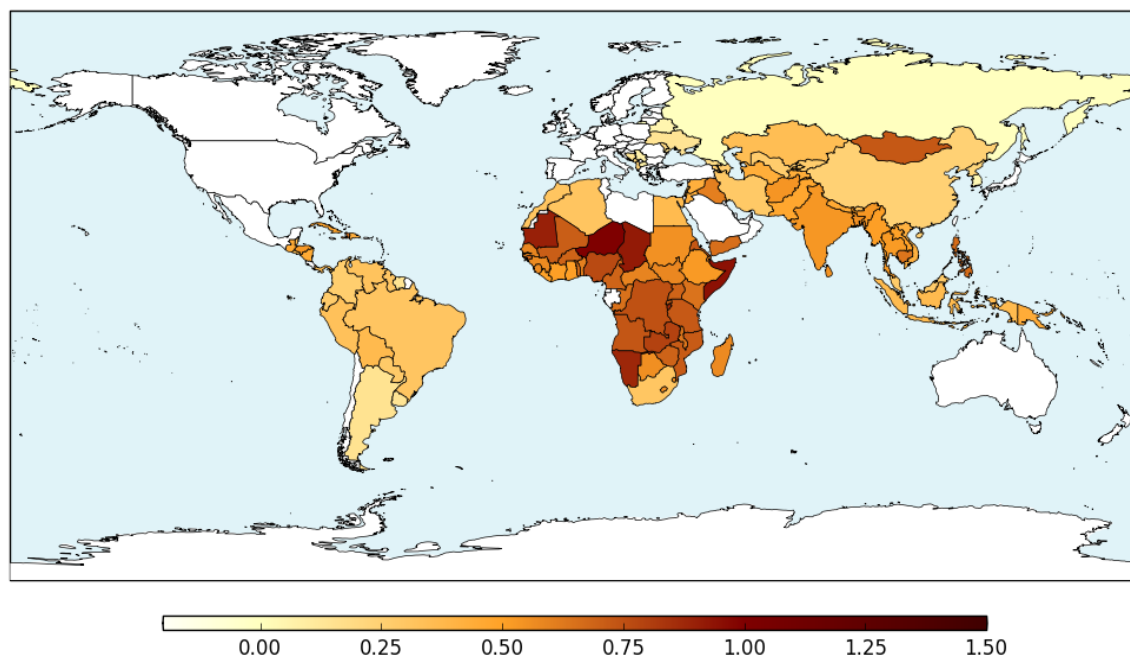


Figure 3 – Present-day vulnerability to food insecurity as measured by the climate and food insecurity index. The colour bar shown is that used on the website, which displays the whole range of index values for all future projections of the index. The present-day index varies from 0 to 1, and therefore only a proportion of the colour bar displayed is used for this map.

3 Future projections of vulnerability to food insecurity

Future projections of the climate and food insecurity index were calculated for a range of scenarios of different future global greenhouse gas emissions and adaptation levels. The greenhouse gas emission scenarios correspond to future projections of the exposure component of the index using climate model projections, whereas the scenarios of adaptation investment correspond to changes in the sensitivity and adaptive capacity components of the index. These future scenarios are described in more detail in the following sections.

3.1 Greenhouse gas emission scenarios

Future projections of the climate and food insecurity index were calculated for three scenarios of global future greenhouse gas emissions: low, medium and high emissions. These three scenarios correspond to climate model projections of the exposure component of the index (a country-level indicator of the average length of flood and drought events constructed from gridded data, see Section 2.1) for three different greenhouse gas concentration pathways. These are the Representative Concentration Pathways (RCPs; van Vuuren *et al.*, 2011) RCP2.6, RCP4.5 and RCP8.5:

- **RCP2.6, the low emissions scenario**, represents a rapid and sustained reduction in future global greenhouse gas emissions, resulting in an increase in global average temperature of around 2°C above pre-industrial values by the end of the 21st century.
- **RCP4.5, the medium emissions scenario**, represents a modest reduction in future global greenhouse gas emissions, resulting in an increase in global average temperature of around 2.5°C - 3°C above pre-industrial levels by the end of the 21st century.
- **RCP8.5, the high emissions scenario**, represents considerable future increases in global greenhouse gas emission resulting, in a rise in global average

temperature of 4°C or more above pre-industrial levels by the end of the 21st century.

The exposure component was calculated using an ensemble of twelve climate models from the Coupled Model Intercomparison Project Phase 5 (CMIP5; Taylor *et al.*, 2012) multi-model ensemble, used to inform the latest Inter-Governmental Panel on Climate Change 5th Assessment Report (IPCC AR5; IPCC, 2013). The twelve models are those that were available for commercial use at the time of study, and have a resolution of 90 latitude grid cells x 144 longitude grid cells or more. The models have a good representation of the range of global average temperature projections from the CMIP5 ensemble. The models and their resolutions are listed in Table 2. Each of the models was re-gridded to the lowest common grid of 90 x 144 grid cells, and the low population and agricultural cropland mask (Figure 2) was also applied.

Table 2 – The twelve CMIP5 models used for the future climate projections, and their resolutions.

Model name	Modelling centre	Number of latitude grid cells	Number of longitude grid cells
BCC-CSM1-1-M	Beijing Climate Center, China Meteorological Administration	160	320
CCSM4	National Center for Atmospheric Research	192	288
CESM1-CAM5	Community Earth System Model Contributors	288	288
CNRM-CM5	Centre National de Recherches Météorologiques / Centre Européen de Recherche et Formation Avancée en Calcul Scientifique	128	256
GFDL-CM3	NOAA Geophysical Fluid Dynamics Laboratory	90	144
GFDL-ESM2G	NOAA Geophysical Fluid Dynamics Laboratory	90	144
GFDL-ESM2M	NOAA Geophysical Fluid Dynamics Laboratory	90	144
HadGEM2-ES	Met Office Hadley Centre	145	192
IPSL-CM5A-MR	Institut Pierre-Simon Laplace	143	144
MPI-ESM-LR	Max-Planck-Institut für Meteorologie	96	192
MPI-ESM-MR	Max-Planck-Institut für Meteorologie	96	192
NorESM1-M	Norwegian Climate Centre	96	144

For each of the climate models, indicators for the average length of flood and drought events per country were calculated for two future time periods: the 2050s (2041-2070) and the 2080s (2071-2100). This was done by adding the model anomaly for each of the future time periods (calculated by subtracting the model baseline (1981-2010) from the model future) to the respective flood and drought indicators from the baseline WATCH data. The indicators were then aggregated to country level by selecting the median value within the country borders (as in the baseline computation, see Section 2.1).

In order to provide a measure of exposure in the context of present-day vulnerability, the future flood and drought country-level indicators were normalised with respect to the maximum and minimum values from the baseline flood and drought indicators. The exposure component was then calculated by summing these normalised future flood and

drought indicators, and normalising with respect to the maximum and minimum values from the baseline exposure component. This resulted in a future measure of exposure that is relative to the baseline measure of exposure, where the values are on a scale of 0 to more than 1. Values greater than 1 indicate an exposure value greater than that seen in the present-day.

In some cases, the climate model projections do not have the required criteria to define a drought in some countries, and therefore there is no exposure component. This only occurs in a few countries and models, and is resolved by excluding these countries from the index calculation for the models in question, resulting in the ensemble mean being based on fewer models for that particular country (see Section 3.3). The specific models and countries are shown in the Food Insecurity & Climate Change Model Spread document, available to download from the website.

3.2 Scenarios of adaptation investment

Two scenarios of adaptation investment were calculated: high and low adaptation. The scenarios represent reductions in how sensitive agricultural production is to climate-related hazards, and increases in capacity to cope with climate-related food shocks, through changing the sensitivity and adaptive capacity components of the index accordingly.

The change is applied to the sensitivity and adaptive capacity component values (not the individual indicators that make up these components) and is dependent on the level of adaptation chosen (low or high). The change is scaled using a logarithmic function which is dependent on the present-day measures of sensitivity and adaptive capacity. This allows countries that have relatively high measures of sensitivity or poor adaptive capacity in the present-day to improve more than those with lower sensitivity or better adaptive capacity, with the same level of adaptation investment.

The change is applied across two future time steps: the 2050s and 2080s. For the 2050s time period, the future value of either the sensitivity or adaptive capacity component per country is given by:

$$x_{2050s} = x_{baseline} - \ln\left(\frac{2 + p - x_{baseline}}{2 - x_{baseline}}\right)$$

where $x_{baseline}$ is the baseline value of sensitivity or adaptive capacity for a given country, and p is the adaptation scenario scaling factor dependent on the level of adaptation:

- $p = 0.1$ for a low level of adaptation,
- $p = 0.2$ for a high level of adaptation.

For the 2080s time period, a further change of p is applied to the 2050s values, so that the future value is given by:

$$x_{2080s} = x_{2050s} - \ln\left(\frac{2 + p - x_{2050s}}{2 - x_{2050s}}\right)$$

If either x_{2050s} or x_{2080s} result in negative values, they are set to be zero as this is deemed to be the lowest plausible value based on the physically plausible limits used for the normalisation in the present-day.

In the 2050s under the high adaptation scenario, this scaled change results in a reduction in sensitivity or improvement in adaptive capacity ranging from approximately 10% in countries with the lowest sensitivity and best adaptive capacity, to approximately

15% in countries with the highest sensitivity and worst adaptive capacity compared to the present-day. In the 2080s, a further change of the same scale (approximately 10-15%) is applied to the 2050s values.

Similarly, for the low adaptation scenario, the scaled change results in a change of approximately 5-10% in the 2050s compared to the present-day, and a further change of approximately 5-10% in the 2080s compared to the 2050s.

The scenario where no adaptation is applied is also available to view on the website. This scenario maintains the sensitivity and adaptive capacity components of the index at the present-day level, .

Other functions for the scaled change and values of the adaptation scenario scaling factor p were tested. Although different functions and scaling factors make changes to the absolute country values, the large scale trend in the index under the different scenarios is not sensitive to these changes.

3.3 The future climate and food insecurity index

For each future scenario, the future exposure, sensitivity and adaptive capacity components were summed together and normalised with respect to the maximum and minimum values from the baseline vulnerability index, to give a relative measure.

The future vulnerability index was calculated for each of the twelve climate models. The ensemble mean was calculated by taking the average vulnerability index value across the ensemble members for each country. The ensemble mean results are those shown on the website. The future index values were capped at a value of 1.5, as values over this threshold were outliers of the distribution.

The range of results across the models for all scenarios is available to download from the website, where the minimum and maximum values across the ensemble members per country are also shown. These are the best and worst case individual country values from across the ensemble members.

4 References

FAO (2014) Food security indicators. Available online at:

http://www.fao.org/economic/ess/ess-fs/ess-fadata/en/#.VCKpjed_qjQ, accessed in December 2013.

IPCC, 2013: Climate Change 2013: The Physical Science Basis. Contribution of Working Group I to the Fifth Assessment Report of the Intergovernmental Panel on Climate Change [Stocker, T.F., D. Qin, G.-K. Plattner, M. Tignor, S.K. Allen, J. Boschung, A. Nauels, Y. Xia, V. Bex and P.M. Midgley (eds.)]. Cambridge University Press, Cambridge, United Kingdom and New York, NY, USA, 1535 pp, doi:10.1017/CBO9781107415324.

Knapp, K. R., M. C. Kruk, D. H. Levinson, H. J. Diamond, and C. J. Neumann, 2010: The International Best Track Archive for Climate Stewardship (IBTrACS): Unifying tropical cyclone best track data. *Bulletin of the American Meteor. Society*, 91, 363-376. non-government domain doi:10.1175/2009BAMS2755.1

Krishnamurthy, P. K., Lewis, K. and Choularton R. J. (2014) A methodological framework for rapidly assessing the impacts of climate risk on national-level food security through a vulnerability index. *Global Environmental Change*, 25, 121-132.

Monfreda, C., Ramankutty, R. and Foley, J. A. (2008). Farming the planet: 2. Geographic distribution of crop areas, yields, physiological types, and net primary production in the year 2000. *Global Biogeochemical Cycles*, 22, GB1022. DOI: 10.1029/2007GB002947

OECD (2011) OECD Regional Typology. OECD: Paris.

Taylor, K.E., R.J. Stouffer, and G.A. Meehl, 2012: An Overview of CMIP5 and the experiment design." *Bull. Amer. Meteor. Soc.*, 93, 485-498, doi:10.1175/BAMS-D-11-00094.1.

van Vuuren, D. P., Lucas, P., and Hilderink, H. (2007) Downscaling drivers of global environmental change. Enabling use of global SRES scenarios at the national and grid levels. *Global Environ Chang*, 17, 114–130.

van Vuuren DP, Edmonds J, Kainuma MLT, Riahi K, Thomson A, Matsui T, Hurtt G, Lamarque J-F, Meinshausen M, Smith S, Grainer C, Rose S, Hibbard KA, Nakicenovic N, Krey V, Kram T. 2011: Representative concentration pathways: An overview. *Climatic Change*. doi:10.1007/s10584-011-0148-z

Wanders, N., Van Lanen, H. A. J., and van Loon, A. F. (2010) Indicators for drought characterization on a global scale. WATCH Technical Report No. 24

Weedon, G. P., Gomes, S., Viterbo, P., Shuttleworth, W. J., Blyth, E., Österle, H. and Best, M. (2011) Creation of the WATCH Forcing Data and Its Use to Assess Global and Regional Reference Crop Evaporation over Land during the Twentieth Century. *Journal of Hydrometeorology*, 12, 5.